


Diagnostic and Prognostic Potential of Multiparametric Renal MRI in Kidney Transplant Patients

Rebeca Echeverria-Chasco, PhD,^{1,2}  Paloma L. Martin-Moreno, MD, PhD,^{2,3*}

Veronica Aramendía-Vidaurreta, PhD,^{1,2}  Leyre Garcia-Ruiz, MEng,^{1,2}

José María Mora-Gutiérrez, MD, PhD,^{2,3} Marta Vidorreta, PhD,⁴ Arantxa Villanueva, PhD,^{2,5,6}

David Cano, MD, PhD,^{1,2} Gorka Bastarrika, MD, PhD,^{1,2} Nuria Garcia-Fernandez, MD, PhD,^{2,3,7}

and Maria A. Fernández-Seara, PhD^{1,2} 

Background: Multiparametric MRI provides assessment of functional and structural parameters in kidney allografts. It offers a non-invasive alternative to the current reference standard of kidney biopsy.

Purpose: To evaluate the diagnostic and prognostic utility of MRI parameters in the assessment of allograft function in the first 3-months post-transplantation.

Study Type: Prospective.

Subjects: 32 transplant recipients (54 ± 17 years, 20 females), divided into two groups according to estimated glomerular filtration rate (eGFR) at 3-months post-transplantation: inferior graft function (IGF; $eGFR < 45$ mL/min/1.73 m², $n = 10$) and superior graft function (SGF; $eGFR \geq 45$ mL/min/1.73 m², $n = 22$). Further categorization was based on the need for hemodialysis (C1) and decrease in s-creatinine (C2) at 1-week post-transplantation: delayed-graft-function (DGF: $n = 4$ C1, $n = 10$ C2) and early graft-function (EGF: $n = 28$ C1, $n = 22$ C2).

Field Strength/Sequence: 3-T, pseudo-continuous arterial spin labeling, T1-mapping, and diffusion-weighted imaging.

Assessment: Multiparametric MRI was evaluated at 1-week in all patients and 3-months after transplantation in 28 patients. Renal blood flow (RBF), diffusion coefficients (ADC, Δ ADC, D , ΔD , D^* , flowing fraction f), T_1 and ΔT_1 were calculated in cortex and medulla. The diagnostic and prognostic value of these parameters, obtained at 3-months and 1-week post-transplantation, respectively, was evaluated in the cortex to discriminate between DGF and EGF, and between SGF and IGF.

Statistical Tests: Logistic regression, receiver-operating-characteristics, area-under-the-curve (AUC), confidence intervals (CIs), analysis-of-variance, t-test, Wilcoxon-Mann-Whitney test, Fisher's exact test, Pearson's correlation. P -value < 0.05 was considered significant.

Results: DGF patients exhibited significantly lower cortical RBF and f and higher D^* . The diagnostic value of MRI for detecting DGF was excellent (AUC = 100%). Significant differences between patients with IGF and SGF were found in RBF, ΔT_1 , and ΔD . Multiparametric MRI showed higher diagnostic (AUC = 95.32%; CI: 88%–100%) and prognostic (AUC = 97.47%, CI: 92%–100%) values for detecting IGF than eGFR (AUC = 89.50%, CI: 79%–100%).

Data Conclusion: Multiparametric MRI may show high diagnostic and prognostic value in transplanted patients, yielding better results compared to eGFR measurements.

Level of Evidence: 2

Technical Efficacy: Stage 1

J. MAGN. RESON. IMAGING 2024.

View this article online at wileyonlinelibrary.com. DOI: 10.1002/jmri.29235

Received Oct 29, 2023, Accepted for publication Dec 27, 2023.

*Address reprint requests to: P.L.M.-M., Department of Nephrology, Clínica Universidad de Navarra, Pio XII, 36, 31008 Pamplona, Spain.

E-mail: plmartin@unav.es

The first two authors share first authorship. The last two authors are Joint last authors.

From the ¹Department of Radiology, Clínica Universidad de Navarra, Pamplona, Navarra, Spain; ²Instituto de Investigación Sanitaria de Navarra (IdiSNA), Pamplona, Navarra, Spain; ³Department of Nephrology, Clínica Universidad de Navarra, Pamplona, Navarra, Spain; ⁴Siemens Healthcare, Madrid, Spain; ⁵Electrical Electronics and Communications Engineering Department, Public University of Navarre, Pamplona, Navarra, Spain; ⁶Smart Cities Institute, Public University of Navarre, Pamplona, Navarra, Spain; and ⁷Red de Investigación Renal (REDINREN) and RICORS2040, Spain

Additional supporting information may be found in the online version of this article

This is an open access article under the terms of the [Creative Commons Attribution-NonCommercial-NoDerivs](https://creativecommons.org/licenses/by-nc-nd/4.0/) License, which permits use and distribution in any medium, provided the original work is properly cited, the use is non-commercial and no modifications or adaptations are made.

Chronic kidney disease (CKD) is a major health problem with increasing prevalence and transplantation is the preferred treatment for patients with kidney failure (CKD Stage 5), offering higher quality of life and longer survival time than dialysis.¹ In the last decades, efforts have been made to preserve allograft function; however, long-term survival remains a challenge.² Survival is affected by several factors. One common problem is delayed graft function (DGF). This is classically defined as the need for hemodialysis during the first week after transplantation and often related to ischemia–reperfusion injury.³ Specifically, DGF is associated with acute tubular necrosis, increased risk of acute rejection, impairment of long-term function, and allograft loss.³ It is estimated that DGF affects 20%–50% of allografts from deceased donors.⁴

Kidney function is evaluated clinically by the estimated glomerular filtration rate (eGFR) based on serum creatinine (s-creatinine). However, poor agreement between eGFR and real GFR in transplant recipients has been reported, as well as low reliability of eGFR for monitoring function over time.⁵ Biopsy remains the reference standard to diagnose the underlying pathology and to plan treatment.⁶ However, it is an invasive procedure (with risk of bleeding, infections, hematomas, and other complications), it cannot be readily repeated in the postoperative period, and suffers from sampling errors.⁶ Imaging techniques employed clinically, such as Doppler ultrasonography, may also present limitations and cannot predict the allograft outcome.^{7,8}

Multiparametric MRI is considered a promising technique that can generate biomarkers associated with perfusion and oxygenation changes, fibrosis, inflammation or edema, among other pathological processes.⁹ Specifically, tissue perfusion can be imaged with arterial spin labeling (ASL),¹⁰ oxygenation can be measured with the blood oxygenation level dependent (BOLD) technique,⁹ and tissue microstructure can be assessed with diffusion-weighted imaging (DWI), a technique sensitive to Brownian motion of water molecules in tissue.¹¹ Intravoxel incoherent motion (IVIM) is a DWI technique that can separate slow tissue diffusion from fast molecular movement associated with blood microcirculation and tubular flow.¹¹ The molecular environment can be evaluated with T1- or T2-mapping sequences.⁹ Moreover, such multiparametric MRI techniques do not require administration of external contrast agents.

Previous studies have assessed the value of MRI to characterize allografts, investigating the associations of MRI parameters with allograft dysfunction^{12–18} and histopathology.^{19–21} Furthermore, ASL or DWI-IVIM studies have shown the potential of MRI to discriminate between patients with DGF and early graft function (EGF).^{18,22} Comparing ASL to BOLD, ASL showed higher diagnostic value for detecting injured allografts, and the combination of both techniques did not improve the performance of ASL alone.¹⁷ Other studies combined DWI, T1-mapping, or ASL to discriminate between

patients with stable or unstable evolution, showing reduced DWI and perfusion parameters in allografts with impaired function^{13,16,18,19,23,24} and prolonged T_1 in dysfunctional and fibrotic allografts.^{19,20} Other studies have reported increased T_1 and reduced corticomedullary difference (CMD) early after transplantation.^{25,26}

The main aims of this study were to investigate changes in perfusion, DWI parameters, and T_1 parameters at two timepoints (first week and 3 months after transplantation), to correlate these parameters with renal function, to assess the diagnostic value of multiparametric MRI, and to evaluate its prognostic potential.

Materials and Methods

The study was approved by the Ethics Research Committee. Written informed consent was obtained from all subjects.

Clinical Assessment and Transplantation Details

Patient and donor demographic data were collected at study entry. Inclusion criteria were adult patients who had undergone a deceased donor kidney transplant. Exclusion criteria were surgical complications and MRI contraindications. Patient clinical data were recorded during 3 months after transplantation following clinical protocols, including s-creatinine and eGFR calculated using the CKD Epidemiology Collaboration (CKD-EPI) equation.²⁷ Pretransplant donor biopsy findings were retrieved in cases where the biopsy had been performed and recipient biopsy data were recorded when available.

During the first week after transplantation, patients were categorized as presenting DGF or EGF. Specifically, DGF was defined according to two criteria: need for hemodialysis during that week (criterion-1) and lack of decrease of s-creatinine by at least 25% during the first 48 hours (criterion-2).²⁸ Subsequently, patients were divided into two groups according to eGFR measured at 3-months post-transplantation: 1) eGFR ≥ 45 mL/min/1.73 m², referred to as superior graft function (SGF), and 2) eGFR < 45 mL/min/1.73 m², referred to as inferior graft function (IGF). An eGFR cut-off of 45 mL/min/1.73 m² was selected because this is considered the threshold between CKD stages 3a and 3b, and previous work has indicated that this threshold may be suitable for predicting favorable long-term transplantation outcomes.²⁹

MRI Protocol

The MRI protocol, described in detail in Echeverría-Chasco et al.,³⁰ was performed at 1-week after surgery (referred to as exam-1) and at 3-months post-transplantation (referred to as exam-2). No specific preparations, such as fasting or fluid intake restrictions, were undertaken before the MRI acquisitions. Sequences were selected so that the exam duration did not exceed 30 minutes to ensure patient comfort. The protocol was performed on a 3-T scanner (Skyra; Siemens Healthcare, Erlangen, Germany) using 32-channel spine and 18-channel body array coils. It included anatomical (T2-weighted half-Fourier acquired single-shot turbo spin echo or HASTE and a T_1 -weighted volumetric interpolated breath-hold examination or VIBE sequences), ASL, DWI-IVIM, and T1-mapping sequences. Sequence parameters are included in Data S1 (section 1). Briefly, tissue perfusion was measured by employing a pseudo-continuous ASL

(PCASL) sequence with presaturation pulses, background suppression, and fat saturation with a spin-echo echo planar imaging (SE-EPI) readout and by acquiring 25 ASL pairs and a proton-density image. Furthermore, T1 mapping was acquired with an inversion recovery sequence employing 14 inversion times (TIs, range: 200–2000 msec), and a fat-suppressed SE-EPI readout. In addition, DWI-IVIM data were acquired with a single-shot EPI readout and spectral attenuated inversion recovery (SPAIR) at 13 b -values (range: 0–800 sec/mm²).

From the acquired data, voxel-wise maps of renal blood flow (RBF), diffusion parameters (apparent diffusion coefficient or ADC, slow diffusion coefficient D , fast diffusion coefficient D^* , and flowing fraction f), and T_1 were computed. All images were acquired in free breathing. In the second MRI exam, the imaging planes covering the kidney acquired in the first study were reproduced.

Image processing was performed in MATLAB (version R2020; The MathWorks Inc., Natick, MA, USA). First, motion was corrected slice-wise in Elastix (version 5.0.1, <https://elastix.lumc.nl/>)³¹ to compensate for respiratory and organ motion. Because of the different image resolutions, ASL and T_1 images were registered simultaneously while for IVIM, intrasequence image registration was performed. Then, MRI parameter maps were calculated as follows:

RENAL BLOOD FLOW. Perfusion-weighted images were computed and averaged. The RBF maps were calculated using the single compartment model.¹¹

T1 MAP. Inversion recovery data were fitted to generate T1 maps.³² T_1 corticomedullary difference (CMD) (ΔT_1) was calculated as $|T_1(\text{cortex}) - T_1(\text{medulla})|$.

IVIM MAPS. D , D^* , and f coefficients were generated from fitting the IVIM bi-exponential model to the signal intensity decay.¹¹ The ADC was generated by fitting the single exponential model¹¹ to DWI data for the b -values >200 and $b = 0$ sec/mm². Furthermore, CMD in D was calculated as follows: $D\text{CMD}(\Delta D) = D(\text{cortex}) - D(\text{medulla})$ and similarly, ADC CMD (ΔADC).

Regions of interest (ROIs) were manually drawn (REC, 5 years of experience) in the cortex and medulla (excluding vascular structures, collecting systems, and cysts) in the T1 maps, based on T_1 differences between the two compartments using ITK-SNAP (Version 4.0.2, www.itksnap.org). These were employed to compute mean cortical and medullary RBF and T_1 . The T_1 CMD (ΔT_1) was calculated as $|T_1(\text{cortex}) - T_1(\text{medulla})|$. The ROIs were also drawn in the IVIM b0-images to compute mean DWI parameters. CMD in D was calculated as: $D\text{CMD}(\Delta D) = D(\text{cortex}) - D(\text{medulla})$ and similarly, ADC CMD (ΔADC). Data S1 (section 2) shows representative segmentations of renal cortical and medullary regions.

Statistical Analysis

Statistical analysis was performed using R software (version 4.3.0.; <https://www.r-project.org/>). Normality tests were applied to each variable. Demographic and clinical variables were compared between groups (DGF vs. EGF and IGF vs. SGF) using unpaired t -test or Wilcoxon–Mann–Whitney test for continuous variables and Fisher’s exact test for categorical variables.

In the statistical analyses of MRI parameters, mean cortical values were evaluated except for ΔT_1 , ΔD , and ΔADC (which measured CMD). To evaluate the diagnostic utility of MRI parameters to detect DGF, differences in parameters recorded in the exam-1 were assessed between EGF and DGF groups using unpaired t -tests or Wilcoxon–Mann–Whitney tests.

Subsequently, binary logistic regression and receiver operating characteristics (ROC) curve analyses were performed. Furthermore, univariate models and two multivariate models were tested, which were designed after variable selection (Data S1 section 3). Model 1 included RBF, D , ΔD , D^* , f , T_1 , and ΔT_1 . Model 2 included RBF, D , ΔD , T_1 , and ΔT_1 . To evaluate model efficiency, the area under the curve (AUC) and confidence intervals (CIs) were calculated. In addition, when the AUC was significantly different from 0.5, Youden-selected thresholds were determined, and sensitivities and specificities were computed.

To evaluate the capacity of MRI parameters to detect and predict IGF, these parameters and eGFR were compared between groups and exams using analysis of variance (ANOVA) for repeated measurements. Non-normal data were transformed with the Aligned-Rank-Transform (ART),³³ and ANOVA was performed on aligned data. Testing by ANOVA included one between-subject factor: group (two levels: IGF and SGF), one within-subject factor: exam (two levels: 1 and 2), and their interaction. Post hoc tests employing t -test or Wilcoxon–Mann–Whitney test with Bonferroni correction compared between-group differences at each timepoint.

Then, binary logistic regression and ROC analyses were performed to evaluate prognostic and diagnostic values of MRI measurements. For diagnostic capability, MRI parameters obtained at 3-months post-transplantation were considered (which were measured on the same day as the eGFR value used to define the groups). For prognostic ability, MRI parameters obtained during exam-1 were used. In both cases, univariate and multivariate models 1 and 2 were tested.

Pairwise correlations between cortical MRI parameters (mean value across visits) and eGFR were evaluated using Pearson’s correlation. In all analyses, a P -value <0.05 was considered statistically significant.

Results

Patient Demographic and Clinical Data

Thirty-two transplant recipients were recruited for the study, 14 of whom received an organ donation after circulatory death (DCD). All underwent exam-1 (time after transplantation: 7 ± 3 days) while 28 completed exam-2 (time: 16 ± 3 weeks), while four patients withdrew from the study but were followed-up clinically. Demographic and clinical characteristics are shown in Table 1.

Pretransplant biopsies were available in 15 cases and first-week post-transplant biopsies were available in three cases. One pretransplant biopsy showed interstitial fibrosis (30%), tubular atrophy (30%), and glomerular sclerosis (12%). The other 14 showed fibrosis equal or lower than 10%, while glomerular sclerosis was 12% in one case and below 10% in the rest. The three post-transplant biopsies

TABLE 1. Demographic and Clinical Data

	All Patients	Criterion 1		Criterion 2		
		EGF	DGF	EGF	DGF	SGF
Recipient Data						
Age (years)	54 ± 17	54 ± 16	52 ± 9	50 ± 15	60 ± 12	49 ± 14
Sex (female)	20 (63%)	16 (57%)	4 (100%)	14 (64%)	6 (20%)	12 (55%)
Donor data						
Age (years)	55 ± 15	54 ± 13	53 ± 13	52 ± 11	59 ± 15	53 ± 11
Sex (female)	14 (44%)	14 (50%)	0 (0%)	13 (59%)	1 (10%) ^a	10 (45%)
BMI	29.9 ± 5.1	26.1 ± 4.8	27.0 ± 2.2	25.2 ± 4.5	28.8 ± 3.7 ^a	26.0 ± 4.5
Donation after circulatory death	14 (44%)	12 (43%)	2 (50%)	7 (32%)	7 (70%)	7 (32%)
Transplantation details						
Cold ischemia time (hours)	17 ± 3	17 ± 4	17 ± 4	17 ± 4	18 ± 3	17 ± 4
Data post-transplantation						
First week						
N	32	28	4	22	10	22
Time between Tx and MRI (days)	7 ± 3	7 ± 3	7 ± 1	6 ± 2	8 ± 3	7 ± 3
eGFR (ml/min/1.73 m ²)	33.5 ± 24.6	41.4 ± 19.2	12.8 ± 7.9	45.3 ± 15.8	21.4 ± 20.0 ^a	46.4 ± 17.5
Third month						
N	28					19
Time between Tx and MRI (days)	19 ± 4					17 ± 4
eGFR (ml/min/1.73 m ²)	49.5 ± 14.6					58.5 ± 10.9
						34.5 ± 7.5 ^a

Values are presented as mean ± SD. eGFR calculated using the Chronic Kidney Disease Epidemiology Collaboration (CKD-EPI) equation. BMI = body mass index; Tx = transplant; eGFR = estimated glomerular filtration rate; EGF = early graft function; DGF = delayed graft function; SGF = superior graft function; IGF = inferior graft function.

^aSignificant differences between groups.

showed inflammatory infiltrate (dense in one and mild in the others). One of them showed interstitial fibrosis, tubular atrophy, and glomerular sclerosis similar to the pretransplant biopsy, while in the other two cases, percentages were low or zero (Supplementary Table S1).

Furthermore, DGF affected 4 patients according to criterion-1 and 10 patients according to criterion-2. The eGFR values were lower in the DGF group. Additionally, when using criterion-2, the DGF group had a lower proportion of female donors and higher donor body mass index. Also, in this case the proportion of DCD was higher in the DGF group (70%) than in the EGF group (32%); however, the difference did not reach statistical significance ($P = 0.06$).

According to eGFR values measured at 3-months post-transplantation, 22 patients showed SGF while 10 presented IGF. From these, 9 in the IGF group and 19 in the SGF group underwent the second MRI acquisitions. The eGFR was lower in the IGF group. The proportion of DCD was higher in the IGF (70%) than in the SGF group (32%), but the difference was not significant ($P = 0.06$).

The proportion of patients with DGF did not differ significantly between IGF and SGF groups, regardless of the criterion used ($P = 0.08$ for criterion-1 and $P = 0.22$ for criterion-2). However, in case of criterion-1, 75% of DGF patients were in the IGF group (Data S1 section 4).

Assessment of DGF

Figure 1 depicts boxplots and Table 2 shows MRI parameter values for each group (DGF vs. EGF) in exam-1. Comparing groups defined following criterion-1, significantly lower RBF values were found in patients with DGF. Using criterion-2, significant reductions in RBF and f were observed, while a significant increase in D^* was found.

Diagnostic Value of MRI Parameters for Detecting DGF

When DGF was defined employing criterion-1, RBF showed high diagnostic value (AUC: 0.9 and CI: 0.69–1.0) with excellent sensitivity (100%) and good specificity (74%). T_1 , ΔT_1 , D^* , and f also showed diagnostic value (Table 3), which

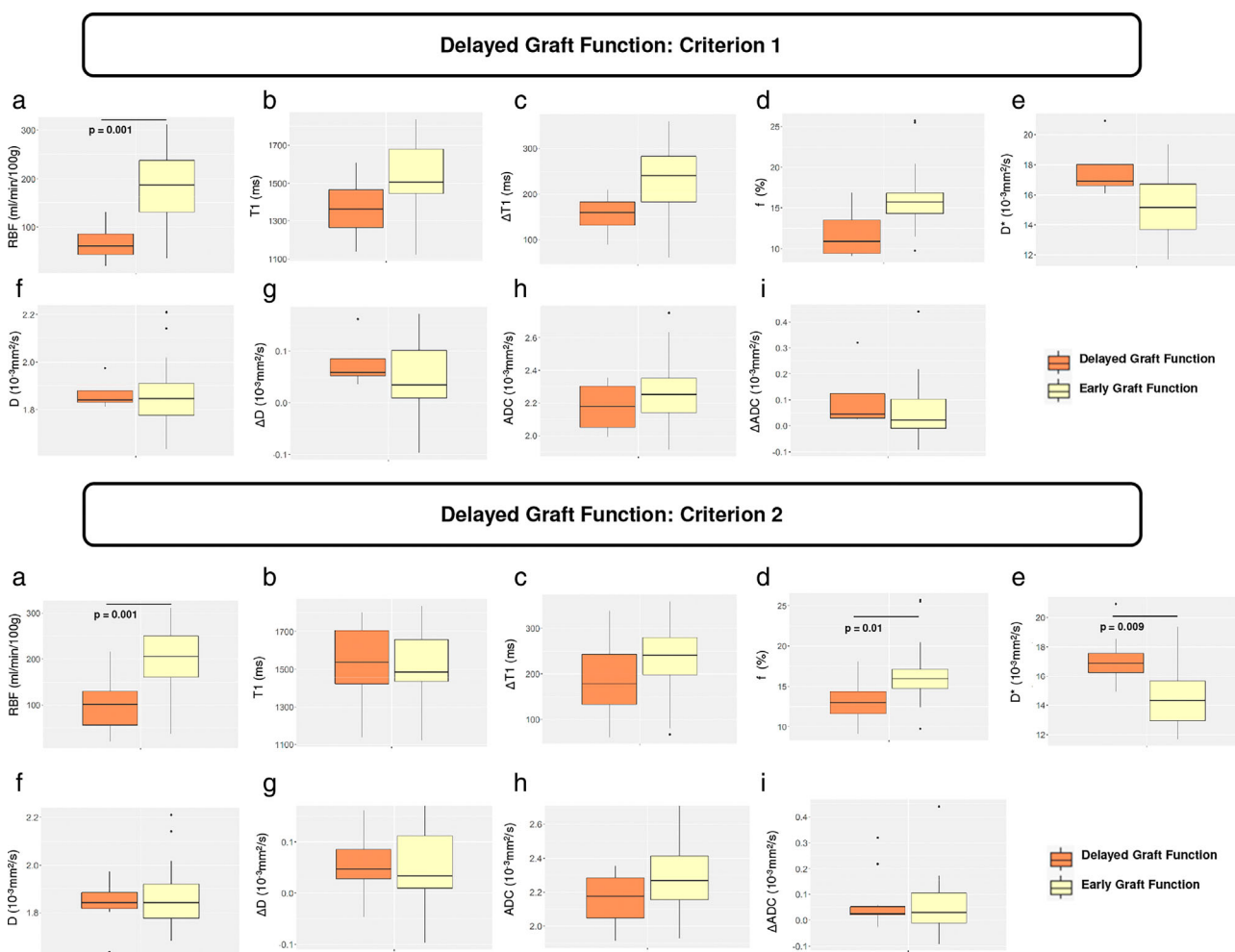


FIGURE 1: Boxplots of cortical MRI parameters measured in the first MRI exam in patients with DGF and EGF. DGF was established based on two criteria (see Methods). (a) RBF, (b) T_1 , (c) T_1 CMD (ΔT_1), (d) flowing fraction, (e) pseudo diffusion coefficient (D^*), (f) diffusion coefficient (D), (g) D CMD (ΔD), (h) ADC, (i) ADC CMD (ΔADC). Significant differences between groups are depicted with their associated P -value.

TABLE 2. Perfusion, Diffusion, and T_1 Parameters Measured in the MRI Exam-1 for Allografts with DGF vs. EGF.

	MRI Exam 1							
	Criterion 1			Criterion 2				
	EGF	DFG	P-Value	EGF	DFG	P-Value		
Perfusion	RBF (mL/minute/100 g)	Cortex	184.64 ± 73.49	68.89 ± 40.31	0.008	200.22 ± 69.47	105.62 ± 60.85	0.001
		Medulla	108.53 ± 33.01	44.19 ± 18.26		111.87 ± 33.70	75.78 ± 35.35	
Diffusion	D (10^{-3} mm ² /sec)	Cortex	1.86 ± 0.13	1.87 ± 0.06		1.86 ± 0.14	1.84 ± 0.08	
		Medulla	1.81 ± 0.13	1.79 ± 0.08		1.81 ± 0.14	1.78 ± 0.08	
	ΔD (10^{-3} mm ² /sec)		0.05 ± 0.07	0.08 ± 0.05		0.05 ± 0.07	0.06 ± 0.06	
	D^* (10^{-3} mm ² /sec)	Cortex	15.11 ± 2.18	17.72 ± 1.88		14.69 ± 2.18	17.10 ± 1.64	0.009
		Medulla	15.31 ± 1.67	16.45 ± 0.92		14.84 ± 1.58	16.80 ± 0.72	
	f (%)	Cortex	16.06 ± 3.47	11.98 ± 3.12		16.63 ± 3.55	13.18 ± 2.76	0.010
		Medulla	15.02 ± 2.86	11.08 ± 2.56		15.67 ± 2.81	12.01 ± 2.10	
ADC (10^{-3} mm ² /sec)	Cortex	2.26 ± 0.20	2.18 ± 0.15		2.29 ± 0.21	2.16 ± 0.14		
	Medulla	2.21 ± 0.21	2.07 ± 0.12		2.24 ± 0.22	2.09 ± 0.12		
	ΔADC (10^{-3} mm ² /sec)		0.05 ± 0.11	0.11 ± 0.12		0.05 ± 0.12	0.07 ± 0.10	
T_1 mapping	T_1 (msec)	Cortex	1555.40 ± 157.42	1368.07 ± 171.07		1530.63 ± 151.99	1532.48 ± 205.72	
		Medulla	1781.41 ± 167.49	1522.41 ± 127.15		1761.35 ± 178.35	1719.94 ± 193.95	
	ΔT_1 (msec)		226.02 ± 81.81	154.34 ± 44.13		230.73 ± 76.91	187.45 ± 83.36	

Values are presented as mean ± SD. P -values for significant between-group comparisons are reported.
EGF = early graft function; DGF = delayed graft function.

TABLE 3. Diagnostic efficiency of MRI parameters for detecting allografts with delayed graft function.

	AUC	CI (95%)	Sensitivity (%)	Specificity (%)
DGF: Criterion 1				
RBF	0.90	0.69–1.0	100	74
D	0.43	0.26–0.88		
ΔD	0.67	0.36–0.98		
f	0.78	0.51–1.0	88.90	75
D^*	0.80	0.53–1.0	67.90	100
ADC	0.60	0.28–0.91		
ΔADC	0.68	0.37–0.99		
ΔT_1	0.78	0.50–1.0	100	63
T_1	0.80	0.52–1.0	93	75
Model 1 (RBF, D , ΔD , D^* , f , T_1 , and ΔT_1)	1.00	1.0–1.0	100	100
Model 2 (RBF, D , ΔD , T_1 , and ΔT_1)	0.95	0.81–1.0	93	100
DGF: Criterion 2				
RBF	0.85	0.68–1.0	86	80
D	0.50	0.28–0.72		
ΔD	0.56	0.34–0.78		
f	0.78	0.59–0.97	77	80
D^*	0.80	0.61–0.98	77	80
ADC	0.67	0.46–0.88		
ΔADC	0.53	0.31–0.75		
ΔT_1	0.65	0.44–0.87		
T_1	0.51	0.29–0.74		
Model 1 (RBF, D , ΔD , D^* , f , T_1 , and ΔT_1)	1.00	1.0–1.0	100	100
Model 2 (RBF, D , ΔD , T_1 , and ΔT_1)	0.86	0.7–1.0	91	70

In bold, AUC values significantly different from 0.5.
AUC = area under the ROC curve; CI = confidence interval.

was increased for the multivariate models, with model 1 yielding excellent classification results (AUC: 1.0 and CI: 1.0–1.0), followed by model 2. Similar results were obtained when DGF was defined according to criterion-2.

Diagnostic and Prognostic Value of MRI Parameters for Detecting IGF

Figure 2 shows MRI parametric maps from two representative patients, in the IGF and SGF groups. Figure 3 depicts boxplots and Table 4 shows eGFR and cortical MRI parameters for each group (IGF vs. SGF) and exam. The ANOVA results indicated significant main effects of exam and group for eGFR. The eGFR values were significantly lower in

patients with IGF compared to SGF and also lower in exam-1 than in exam-2. For RBF, there was a significant effect of group, with lower RBF values in the IGF than the SGF group. For T_1 , there was a significant effect of exam, but post hoc tests were not significant ($P = 0.11$). Furthermore, ΔT_1 showed significant effects of exam and group, which were confirmed by post hoc tests, revealing significantly smaller ΔT_1 in IGF than SGF allografts and in exam-1 than exam-2. The ΔD exhibited significant main effects of exam and group, with higher ΔD in exam-1 and in patients with IGF.

Table 5 shows ROC analyses results for diagnostic value, and Fig. 4a depicts ROC curves of cortical RBF and

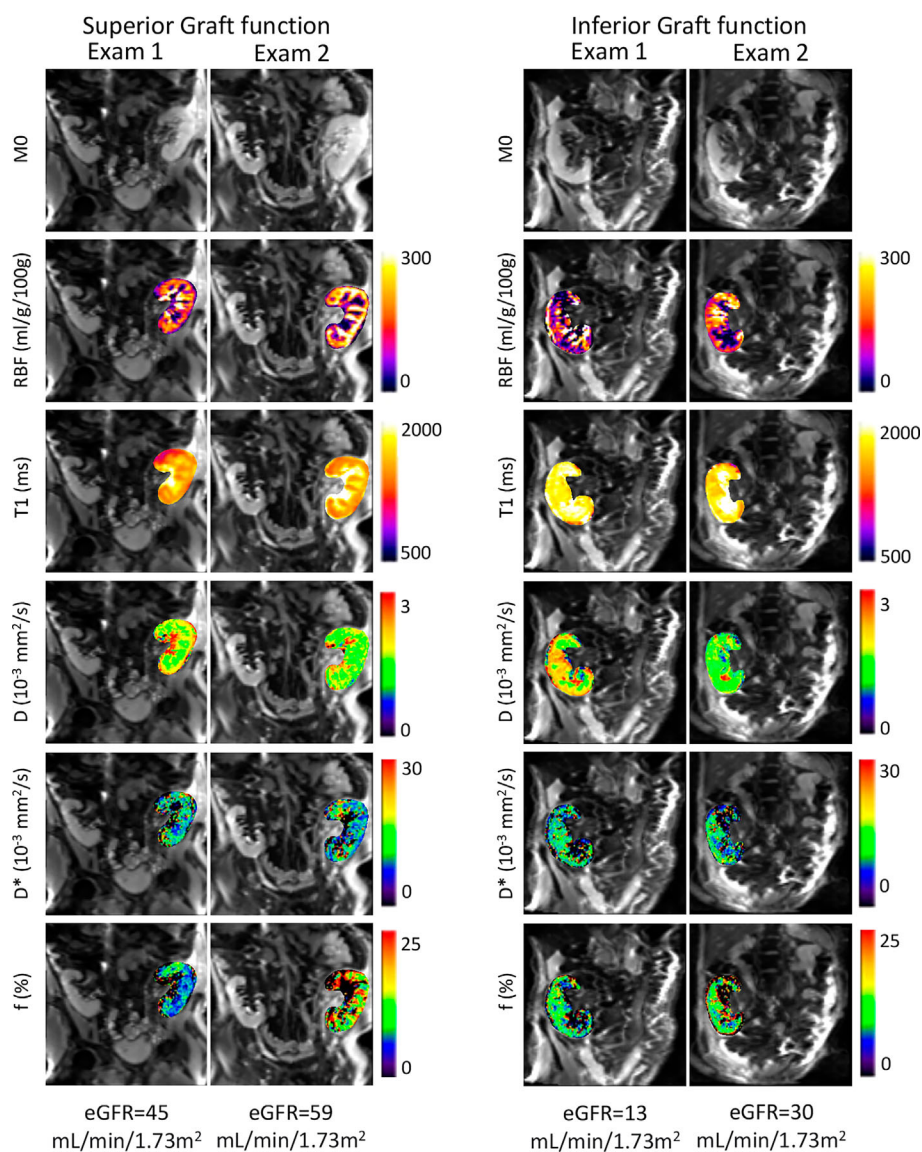


FIGURE 2: Representative MRI images for all quantitative parameter maps obtained in a patient with SGF and a patient with IGF in both MRI exams. The images arranged from top to bottom include M0, RBF, T_1 , D , D^* , and f maps. The eGFR ($\text{mL}/\text{min}/1.73\text{m}^2$) was 45 (MRI exam 1) and 59 (MRI exam 2) for the SGF patient and 13 (MRI exam 1) and 30 (MRI exam 2) for the IGF patient.

multivariate models 1 and 2. The diagnostic value of eGFR was not tested as it was employed to generate the groups. Specifically, RBF showed good diagnostic results with $\text{AUC} = 0.84$ (CI: 0.69–0.98), and high specificity (95%) but lower sensitivity (67%), while multivariate models showed higher AUC (0.95, CI: 0.88–1.00), with high sensitivity and specificity (Table 5, Fig. 4a).

When the prognostic value was evaluated (Table 5), eGFR measured during the first week predicted IGF at 3-months post-transplantation with a high prognostic value ($\text{AUC}: 0.89$ and CI: 0.79–1.00). Among MRI parameters, RBF yielded similar results ($\text{AUC}: 0.90$ and CI: 0.80–1.00), followed by ΔT_1 (Table 5). However, both multivariate models improved the results, with model 1 yielding excellent predictions ($\text{AUC}: 0.97$ and CI: 0.92–1.00), 100% sensitivity, and 86% specificity (Fig. 4b).

Correlations of MRI Parameters with eGFR

There were significant correlations between eGFR and cortical RBF ($r = 0.65$) and ΔT_1 ($r = 0.37$; Fig. 5). However, eGFR did not correlate significantly with DWI parameters or T_1 (P values for T_1 ($P = 0.94$), D ($P = 0.75$), D^* ($P = 0.98$), f ($P = 0.20$), and ΔD ($P = 0.75$)).

Discussion

This study employed multiparametric MRI in transplant patients, enabling quantification of perfusion, DWI, and T_1 parameters. The results showed its diagnostic utility to detect DGF, and diagnostic and prognostic utility to detect IGF at 3 months after the transplantation had been performed.

Commonly, DGF occurs early after transplantation and has high impact on the graft outcome.³⁴ Definitions of DGF

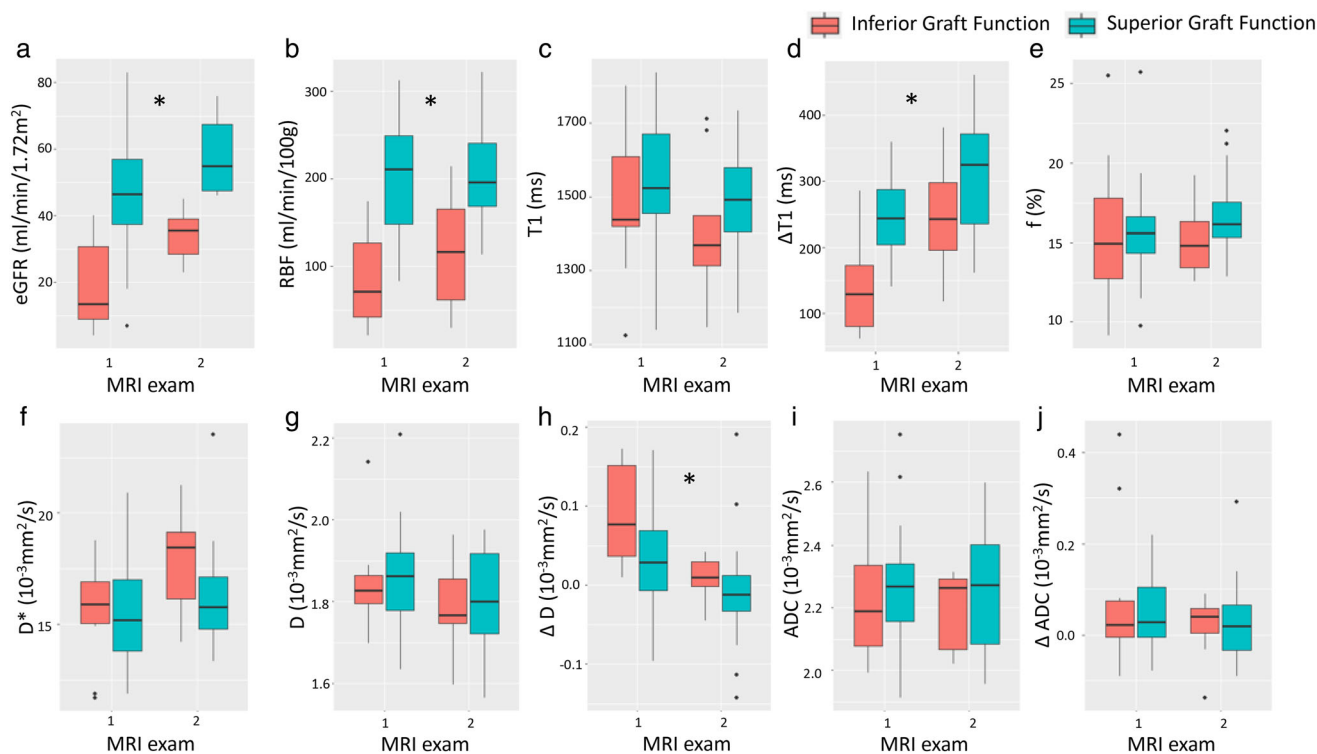


FIGURE 3: Boxplots of eGFR and MRI parameters of IGF group (patients with eGFR <45 mL/min/1.72 m²) (in red) and SGF group (patients with eGFR ≥45 mL/min/1.72 m²) (in blue) measured in the two examinations: (a) eGFR, (b) RBF, (c) T₁ values, (d) T₁ CMD (ΔT₁), (e) flowing fraction, (f) pseudo diffusion coefficient (D*), (g) diffusion coefficient (D), (h) D CMD (ΔD), (i) ADC, and (j) ADC CMD (ΔADC). * Indicates significant differences between groups.

vary in the literature, so here we adopted two different ones: criterion-1, based on dialysis requirement, and criterion-2, based on changes in creatinine, which yielded a larger number of DGF patients.³⁴ Among risk factors for DGF is DCD,³⁵ due to effects of warm ischemia. In our study, the proportion of DCD was higher in the DGF group, although the difference did not reach statistical significance probably due to the low patient number in this group, especially when DGF was defined according to criterion-1.

The interest in developing novel biomarkers to diagnose DGF non-invasively is high, because these patients are in the early postoperative period.³⁶ In our study, RBF was significantly lower in the DGF group and showed the highest diagnostic efficiency. These results are in agreement with the study of Hueper et al, which found impaired perfusion in patients with DGF.³⁷ Specifically in this study, D^* and f , the DWI parameters that are considered more sensitive to microvascular and tubular flow changes, showed significant differences between groups using criterion-2 and presented diagnostic value. Therefore, DGF appeared to be associated with reductions in RBF and f along with increases in D^* . These findings could be explained by the importance of the ischemia-induced damage to the kidney tubules, a primary cause of DGF, albeit not the only one.³⁵

Multivariate models provided very good detection performance regarding DGF, indicating that all MRI parameters

gave information on pathophysiological changes affecting early allograft function. These findings suggest that multiparametric MRI could facilitate DGF detection. Recent studies have consistently associated DGF with poor allograft outcome.^{38,39} Morath et al in a large study on kidney transplantation, reported a lower proportion of patients with good function at 1-year post-transplantation in the DGF group (37%) when compared to the group without DGF (55%), a value that was further reduced when DGF was associated with acute rejection (27%).³⁹ In agreement with such previous work, our study found higher proportion of DGF patients with IGF at 3-months post-transplantation than with SGF, potentially indicating the persistent impact of early functional impairment, although the difference was not statistically significant, probably due to the sample size.

Few prior studies have evaluated diagnostic performance of multiparametric MRI to detect graft dysfunction beyond the early period after transplantation.¹⁶ In our study, kidney recipients were followed-up for up to 3 months and classified into two groups based on eGFR measured at this timepoint. Results showed significantly lower RBF in IGF than in SGF groups, and RBF yielded high diagnostic and prognostic value. Previous studies including ASL and IVIM have also found reduced RBF in allografts with long term dysfunction, reporting high diagnostic efficiency.¹⁶ However, results

TABLE 4. Perfusion, Diffusion, and T_1 Parameters Measured in IGF and SGF Groups, Reported by MRI Exam.

	MRI Exam 1			MRI Exam 2			P-Value
	SGF	IGF	IGF	SGF	IGF	IGF	
Perfusion	RBF (mL/min/100 g)	Cortex	202.53 ± 64.45	89.46 ± 53.68	205.81 ± 57.23	114.17 ± 66.78	<0.001
		Medulla	109.15 ± 31.95	78.42 ± 43.06	94.24 ± 41.54	67.17 ± 41.79	
Diffusion	D (10^{-3} mm ² /sec)	Cortex	1.86 ± 0.13	1.85 ± 0.11	1.81 ± 0.12	1.79 ± 0.10	0.040
		Medulla	1.82 ± 0.14	1.76 ± 0.10	1.82 ± 0.13	1.78 ± 0.10	
	ΔD (10^{-3} mm ² /sec)		0.04 ± 0.06	0.09 ± 0.06	-0.01 ± 0.07	0.01 ± 0.03	
	D^* (10^{-3} mm ² /sec)	Cortex	15.39 ± 2.39	15.54 ± 2.13	16.29 ± 2.23	17.90 ± 2.10	
		Medulla	15.11 ± 1.60	16.22 ± 1.45	15.96 ± 2.40	17.58 ± 2.01	
	f (%)	Cortex	15.55 ± 3.10	15.56 ± 4.73	16.85 ± 2.37	15.31 ± 2.05	
		Medulla	14.74 ± 2.73	14.05 ± 3.77	15.19 ± 1.95	14.28 ± 2.23	
	ADC (10^{-3} mm ² /sec)	Cortex	2.26 ± 0.20	2.24 ± 0.20	2.27 ± 0.19	2.19 ± 0.12	
		Medulla	2.21 ± 0.21	2.16 ± 0.19	2.24 ± 0.20	2.17 ± 0.13	
	Δ ADC (10^{-3} mm ² /sec)		0.05 ± 0.08	0.08 ± 0.16	0.03 ± 0.09	0.02 ± 0.07	
T1 mapping	T_1 (msec)	Cortex	1551.00 ± 154.85	1482.89 ± 197.56	1477.47 ± 131.33	1416.54 ± 170.82	0.006
		Medulla	1798.52 ± 151.81	1624.47 ± 198.68	1784.53 ± 98.27	1671.08 ± 182.76	
	ΔT_1 (msec)		247.52 ± 61.73	141.59 ± 75.19	307.06 ± 84.29	254.54 ± 79.49	

Values are presented as mean ± SD. P-values for significant between-group comparisons are reported. SGF = superior graft function; IGF = inferior graft function.

TABLE 5. Diagnostic and Prognostic Utility of MRI and eGFR in Assessing Graft Function

(A) Diagnostic efficacy of MRI parameters acquired in exam-2 (month-3 after the transplantation) for detecting IGF

MRI Parameters

	AUC	CI (95%)	Sensitivity (%)	Specificity (%)
RBF	0.84	0.69–0.98	67	95
D	0.58	0.35–0.80		
ΔD	0.67	0.46–0.88		
f	0.68	0.44–0.91		
D^*	0.73	0.49–0.96		
ADC	0.64	0.43–0.85		
ΔADC	0.55	0.32–0.78		
T_1	0.67	0.46–0.88		
ΔT_1	0.66	0.45–0.87		
Model 1 (RBF, D , ΔD , D^* , f , T_1 , and ΔT_1)	0.95	0.88–1	90	89
Model 2 (RBF, D , ΔD , T_1 , and ΔT_1)	0.95	0.88–1	89	90

(B) Prognostic efficacy of eGFR and MRI parameters measured in exam-1 (first week after the transplantation) for detecting IGF

Clinical and MRI Parameters

	AUC	CI (95%)	Sensitivity (%)	Specificity (%)
eGFR	0.90	0.79–1	90	89
MRI Parameters				
RBF	0.90	0.80–1.0	78	86
D	0.61	0.40–0.83		
ΔD	0.68	0.48–0.88		
f	0.58	0.32–0.85		
D^*	0.51	0.27–0.75		
ADC	0.60	0.36–0.83		
ΔADC	0.59	0.35–0.82		
T_1	0.67	0.46–0.88		
ΔT_1	0.85	0.67–1.0	78	91
Model 1 (RBF, D , ΔD , D^* , f , T_1 , and ΔT_1)	0.97	0.92–1.0	100	86
Model 2 (RBF, D , ΔD , T_1 , and ΔT_1)	0.95	0.88–1.0	100	82

In bold, AUC values significantly different from 0.5. For these cases, sensitivity and specificity are reported. AUC = area under the ROC curve; CI = confidence interval.

differed regarding the benefit of adding DWI parameters to the classification model. Specifically, one study reported improved results,¹⁸ whereas in another no significant differences were found.¹⁶ Our findings may confirm the superior

classification performance of RBF; however, the multivariate model including IVIM and T_1 improved diagnostic results.

Diagnostic performance of IVIM and T_1 to detect allograft dysfunction associated to fibrosis has also been studied,

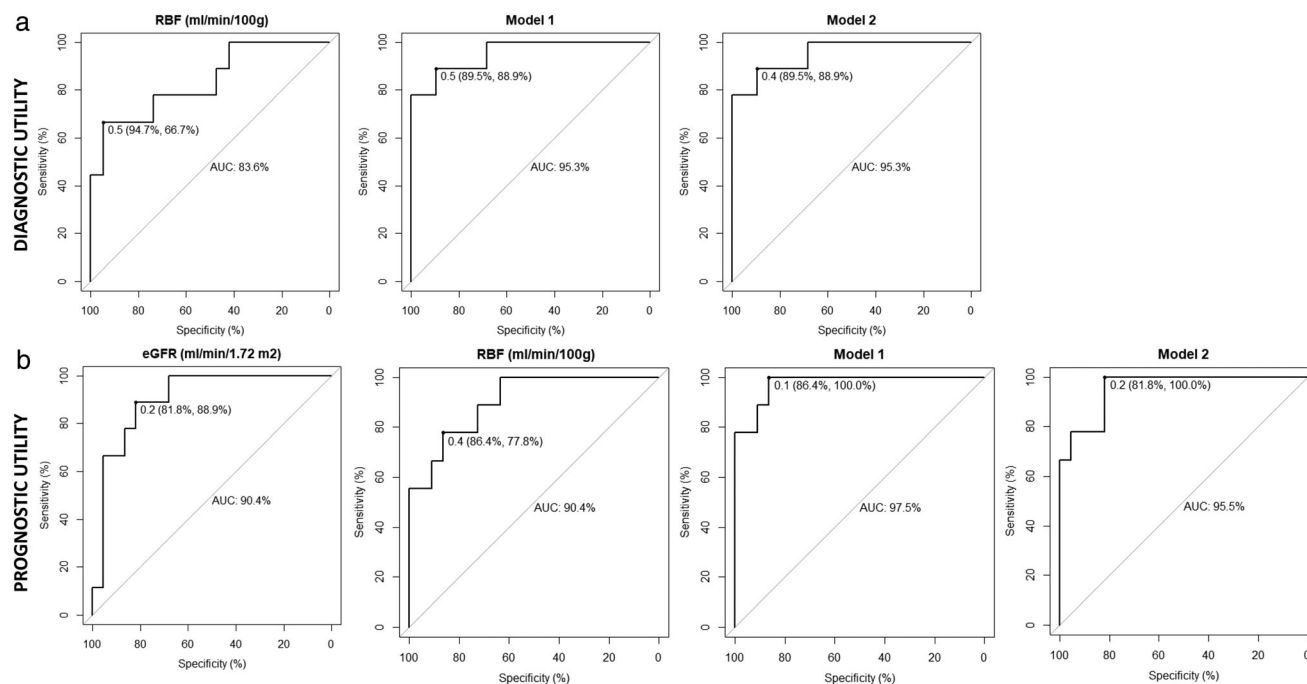


FIGURE 4: Diagnostic and prognostic utility of MRI and eGFR in assessing graft function. (a) Diagnostic utility of MRI in distinguishing between inferior and SGF. ROC curves calculated for RBF and two multivariate models considering a combination of MRI parameters: model 1 (including RBF, D , D CMD, D^* , f , T_1 , and ΔT_1) and model 2 (including RBF, D , D CMD, T_1 , and ΔT_1) for the parameters measured in exam-2. (b) Prognostic utility of eGFR and MRI parameters for distinguishing between inferior and SGF. ROC curves for eGFR, RBF, and two multivariate models considering a combination of MRI parameters: model 1 (including RBF, D , D CMD, D^* , f , T_1 , and ΔT_1) and model 2 (including RBF, D , D CMD, T_1 , and ΔT_1) for the parameters measured in exam-1.

showing good results for T_1 and ADC and their CMD.^{20,25} Although IVIM coefficients D and f correlated with Banff scores, they did not improve the diagnostic performance of ADC for diagnosing chronic dysfunction.²⁵ In our study, T_1 CMD was significantly reduced in allografts with IGF, while D CMD was increased. However, when considered individually, these parameters lacked diagnostic value. Although the presence of fibrosis was not assessed at 3-months post-transplantation, available pre- and post-transplant biopsies did not show fibrosis in the majority of allografts. As fibrosis arises progressively after transplantation,⁴⁰ it is likely that at 3-months post-transplantation the percentage of allografts with fibrosis was still low, which could explain the poor

diagnostic performance of T_1 and DWI parameters individually, as they appear to be more sensitive to this microstructural change.

Prognostic utility of MRI for predicting allograft dysfunction has been scarcely addressed. In the study of Yu et al ASL alone and in combination with IVIM yielded moderate results, which were surpassed by eGFR.¹⁶ Our findings, however, showed good predictive power of RBF, followed by ΔT_1 . In addition, the combination of MRI parameters outperformed eGFR. These results, if confirmed in larger studies, could have important clinical implications, since a prognostic tool could support clinical decision making such as considering changes in immunosuppressive treatment or adding drugs

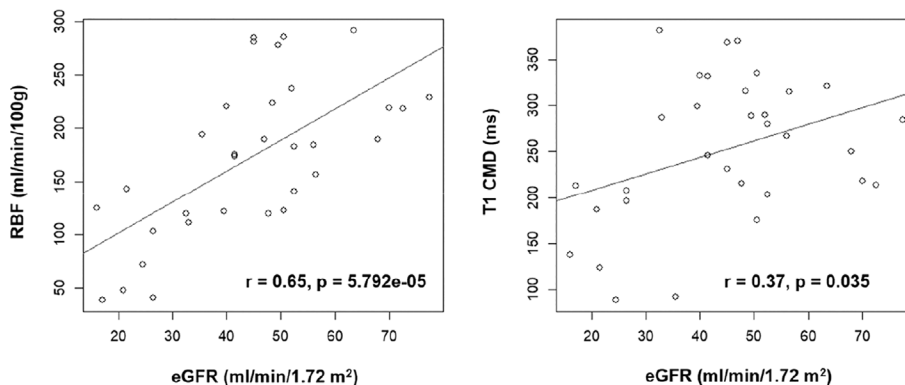


FIGURE 5: Scatter plots and regression lines of: (a) eGFR and cortical perfusion (RBF) ($r = 0.65$) and (b) eGFR and T_1 CMD ($r = 0.37$).

with nephroprotective effects, so that the evolution of the allograft could be improved.

Finally, we observed a strong positive correlation between RBF and eGFR and a moderate correlation between T_1 CMD and eGFR, suggesting that these two parameters were more closely associated to renal function than DWI parameters during the post-transplant period covered by this study.

Limitations

The small sample size of this study is a major limitation, which could have caused an overfitting effect in the multivariate models. Further studies in larger groups of patients are warranted to refine the performance results for MRI biomarkers. Additionally, histopathology data from post-transplant biopsy were not available at 3-months post-transplantation, which would have allowed assessment of underlying pathology in dysfunctional allografts and evaluation of correlations between histology and MRI. Finally, the multiparametric protocol did not include other techniques such as BOLD and T2-mapping, which could contribute to MRI diagnostic and prognostic value, which was due to MRI examination duration constraints.

Conclusion

Diagnostic and prognostic utility of multiparametric MRI for detecting DGF and IGF was evaluated in this study. Specifically, MRI may show high diagnostic and prognostic value for detecting IGF.

Funding Information

This work was funded by Government of Navarra, Grant Number: PC181-182 RM-RENAL. Rebeca Echeverria-Chasco received PhD grant support from Siemens Healthcare Spain.

Conflict of Interest

Marta Vidorreta is an employee of Siemens Healthcare Spain. The authors declare no other conflicts of interest.

References

- Kaballo MA, Canney M, O'Kelly P, Williams Y, O'Seaghda CM, Conlon PJ. A comparative analysis of survival of patients on dialysis and after kidney transplantation. *Clin Kidney J* 2017;11:389-393.
- Martin Moreno PL, Garcia Fernandez N, Lavilla Royo FJ, Mora Gutiérrez JM, Errasti Goenaga P. More than 1000 kidney transplants performed in Pamplona, Navarra: Data from the collaborative transplant study. *Transplant Proc* 2016;48:2891-2894.
- Perico N, Cattaneo D, Sayegh MH, Remuzzi G. Delayed graft function in kidney transplantation. *Lancet (London, England)* 2004;364:1814-1827.
- Wu WK, Famure O, Li Y, Kim SJ. Delayed graft function and the risk of acute rejection in the modern era of kidney transplantation. *Kidney Int* 2015;88:851-858.
- Porrini E, Ruggenenti P, Luis-Lima S, et al. Estimated GFR: Time for a critical appraisal. *Nat Rev Nephrol* 2019;15:177-190.
- Schwarz A, Gwinner W, Hiss M, Rademacher J, Mengel M, Haller H. Safety and adequacy of renal transplant protocol biopsies. *Am J Transplant* 2005;5:1992-1996.
- Jehn U, Schuette-Nuetgen K, Kentrup D, Hoerr V, Reuter S. Renal allograft rejection: Noninvasive ultrasound- and MRI-based diagnostics. *Contrast Media Mol Imaging* 2019;2019:3568067.
- Heaf JG, Iversen J. Uses and limitations of renal scintigraphy in renal transplantation monitoring. *Eur J Nucl Med* 2000;27:871-879.
- Selby NM, Blankestijn PJ, Boor P, et al. Magnetic resonance imaging biomarkers for chronic kidney disease: A position paper from the European Cooperation in Science and Technology action PARENCHIMA. *Nephrol Dial Transplant* 2018;33:4-14.
- Nery F, Buchanan CE, Hartevelde AA, et al. Consensus-based technical recommendations for clinical translation of renal ASL MRI. *Magn Reson Mater Phys Biol Med* 2020;33:141-161.
- Ljimini A, Caroli A, Laustsen C, et al. Consensus-based technical recommendations for clinical translation of renal diffusion-weighted MRI. *Magn Reson Mater Phys Biol Med* 2020;33:177-195.
- Chen L, Ren T, Zuo P, Fu Y, Xia S, Shen W. Detecting impaired function of renal allografts at the early stage after transplantation using intravoxel incoherent motion imaging. *Acta Radiol* 2018;60:1039-1047.
- Wang Y, Li Y, Yin L, Pu H, Chen J-Y. Functional assessment of transplanted kidneys with magnetic resonance imaging. *World J Radiol* 2015;7:343-349.
- Kaul A, Sharma RK, Gupta RK, et al. Assessment of allograft function using diffusion-weighted magnetic resonance imaging in kidney transplant patients. *Saudi J Kidney Dis Transpl* 2014;25:1143-1147.
- Yu YM, Ni QQ, Wang ZJ, Chen ML, Zhang LJ. Multiparametric functional magnetic resonance imaging for evaluating renal allograft injury. *Korean J Radiol* 2019;20:894-908.
- Yu YM, Wang W, Wen J, Zhang Y, Lu GM, Zhang LJ. Detection of renal allograft fibrosis with MRI: Arterial spin labeling outperforms reduced field-of-view IVIM. *Eur Radiol* 2021;31:6696-6707.
- Peng J, Hong Y, Zhu F, Li Y, Luo S, Lu G. A clinical study of using ROC to compare the efficiency of ASL and BOLD in diagnosis of renal allograft function. *Transl Androl Urol* 2023;12:612-621.
- Ren T, Wen C-LL, Chen L-HH, et al. Evaluation of renal allografts function early after transplantation using intravoxel incoherent motion and arterial spin labeling MRI. *Magn Reson Imaging* 2016;34:908-914.
- Bane O, Hectors S, Gordic S, et al. Multiparametric magnetic resonance imaging shows promising results to assess renal transplant dysfunction with fibrosis. *Physiol Behav* 2020;97:414-420.
- Friedli I, Crowe LA, Berchtold L, et al. New magnetic resonance imaging index for renal fibrosis assessment: A comparison between diffusion-weighted imaging and T1 mapping with histological validation. *Sci Rep* 2016;6:1-15.
- Steiger P, Barbieri S, Kruse A, Ith M, Thoeny HC. Selection for biopsy of kidney transplant patients by diffusion-weighted MRI. *Eur Radiol* 2017;27:4336-4344.
- Chang YC, Tsai YH, Chung MC, et al. Intravoxel incoherent motion-diffusion-weighted MRI for investigation of delayed graft function immediately after kidney transplantation. *Biomed Res Int* 2022;2022:1-9.
- Eisenberger U, Thoeny HC, Binser T, et al. Evaluation of renal allograft function early after transplantation with diffusion-weighted MR imaging. *Eur Radiol* 2010;20:1374-1383.
- Palmucci S, Mauro LA, Veroux P, et al. Magnetic resonance with diffusion-weighted imaging in the evaluation of transplanted kidneys: Preliminary findings. *Transplant Proc* 2011;43:960-966.
- Adams LC, Bressemer KK, Scheibl S, et al. Multiparametric assessment of changes in renal tissue after kidney transplantation with quantitative MR relaxometry and diffusion-tensor imaging at 3 T. *J Clin Med* 2020;9:1-16.

26. Peperhove M, Vo Chieu VD, Jang MS, et al. Assessment of acute kidney injury with T1 mapping MRI following solid organ transplantation. *Eur Radiol* 2018;28:44-50.
27. Levey AS, Stevens LA, Schmid CH, et al. A new equation to estimate glomerular filtration rate. *Ann Intern Med* 2009;150:604-612.
28. Yarlagadda SG, Coca SG, Garg AX, et al. Marked variation in the definition and diagnosis of delayed graft function: A systematic review. *Nephrol Dial Transplant* 2008;23:2995-3003.
29. Baek CH, Kim H, Yang WS, Han DJ, Park SK. A postoperative 1-year eGFR of more than 45 ml/min may be the cutoff level for a favorable long-term prognosis in renal transplant patients. *Ann Transplant* 2016; 21:439-447.
30. Echeverria-Chasco R, Martin-Moreno PL, Garcia-Fernandez N, et al. Multiparametric renal magnetic resonance imaging: A reproducibility study in renal allografts with stable function. *NMR Biomed* 2023;36: e4832.
31. Huizinga W, Poot DHJ, Guyader JM, et al. PCA-based groupwise image registration for quantitative MRI. *Med Image Anal* 2016;29: 65-78.
32. Dekkers IA, de Boer A, Sharma K, et al. Consensus-based technical recommendations for clinical translation of renal T1 and T2 mapping MRI. *Magn Reson Mater Phys Biol Med* 2020;33:163-176.
33. Wobbrock JO, Findlater L, Gergle D, Higgins JJ. The aligned rank transform for nonparametric factorial analyses using only anova procedures. *Proc SIGCHI Conf hum factors Comput Syst*. New York, NY, USA, NY, USA: Association for Computing Machinery; 2011. p 143-146.
34. Yarlagadda SG, Coca SG, Formica RNJ, Poggio ED, Parikh CR. Association between delayed graft function and allograft and patient survival: A systematic review and meta-analysis. *Nephrol Dial Transplant* 2008; 24:1039-1047.
35. Nashan B, Abbud-Filho M, Citterio F. Prediction, prevention, and management of delayed graft function: Where are we now? *Clin Transplant* 2016;30:1198-1208.
36. Di W, Ran Q, Yang H, et al. Use of graft-derived cell-free DNA as a novel biomarker to predict allograft function after kidney transplantation. *Int J Urol* 2021;28:1019-1025.
37. Hueper K, Gueler F, Bräsen JH, et al. Functional MRI detects perfusion impairment in renal allografts with delayed graft function. *Am J Physiol Ren Physiol* 2015;308:F1444-F1451.
38. Redfield RR, Scalea JR, Zens TJ, et al. Predictors and outcomes of delayed graft function after living-donor kidney transplantation. *Transpl Int* 2016;29:81-87.
39. Morath C, Döhler B, Kälble F, Pego L. Pre-transplant HLA antibodies and delayed graft function in the current era of kidney transplantation. *Front Immunol* 2020;11:1-10.
40. Cosio FG, Grande JP, Larson TS, et al. Kidney allograft fibrosis and atrophy early after living donor transplantation. *Am J Transplant* 2005; 5:1130-1136.